

Small-bowel MRI in children and young adults with Crohn disease: retrospective head-to-head comparison of contrast-enhanced and diffusion-weighted MRI

Henning Neubauer · Thomas Pabst · Anke Dick ·
Wolfram Machann · Laura Evangelista ·
Clemens Wirth · Herbert Köstler · Dietbert Hahn ·
Meinrad Beer

Received: 11 March 2012 / Revised: 13 July 2012 / Accepted: 8 August 2012 / Published online: 5 December 2012
© Springer-Verlag 2012

Abstract

Background Small-bowel MRI based on contrast-enhanced T1-weighted sequences has been challenged by diffusion-weighted imaging (DWI) for detection of inflammatory bowel lesions and complications in patients with Crohn disease.

Objective To evaluate free-breathing DWI, as compared to contrast-enhanced MRI, in children, adolescents and young adults with Crohn disease.

Materials and methods This retrospective study included 33 children and young adults with Crohn disease ages 17 ± 3 years (mean \pm standard deviation) and 27 matched controls who underwent small-bowel MRI with contrast-enhanced T1-weighted sequences and DWI at 1.5 T. The detectability of Crohn manifestations was determined. Concurrent colonoscopy as reference was available in two-thirds of the children with Crohn disease.

Results DWI and contrast-enhanced MRI correctly identified 32 and 31 patients, respectively. All 22 small-bowel lesions and all Crohn complications were detected. False-positive findings (two on DWI, one on contrast-enhanced MRI), compared to colonoscopy, were a result of large-

bowel lumen collapse. Inflammatory wall thickening was comparable on DWI and contrast-enhanced MRI. DWI was superior to contrast-enhanced MRI for detection of lesions in 27% of the assessed bowel segments and equal to contrast-enhanced MRI in 71% of segments.

Conclusion DWI facilitates fast, accurate and comprehensive workup in Crohn disease without the need for intravenous administration of contrast medium. Contrast-enhanced MRI is superior in terms of spatial resolution and multiplanar acquisition.

Keywords Crohn disease · Diffusion-weighted imaging · Paediatric · Contrast medium · MRI

Introduction

Crohn disease is a chronic inflammatory bowel disorder with a significant incidence and prevalence in children and young adults. Age-specific incidence in paediatric populations is estimated at 16 cases per 100,000 persons [1]. Children and adolescents compose about 15% to 30% of the total population with Crohn disease [2, 3]. Noninvasive imaging modalities free of ionizing radiation have therefore been a particular focus of ongoing research and clinical evaluation in young patients with Crohn disease, who may accumulate high radiation doses with repeated barium fluoroscopy or CT studies over their life-time [4, 5]. US is usually performed as first-line imaging in children with suspected Crohn disease [6]. MRI for Crohn disease was introduced in the early 1990s [7, 8]. With technical advances in scanner hardware and software, MRI has become a valuable diagnostic tool for comprehensive abdominal imaging

H. Neubauer (✉) · L. Evangelista · C. Wirth · M. Beer
Institute of Radiology, Department of Paediatric Radiology,
University Hospital Wuerzburg,
Josef-Schneider-Straße 2,
97080 Wuerzburg, Germany
e-mail: neubauer@roentgen.uni-wuerzburg.de

T. Pabst · W. Machann · H. Köstler · D. Hahn
Institute of Radiology, University Hospital Wuerzburg,
97080 Wuerzburg, Germany

A. Dick
Department of Paediatrics, University Hospital Wuerzburg,
97080 Wuerzburg, Germany

in those children and young adults with Crohn disease [9] in whom US does not provide all the required diagnostic information. The correlation between MRI and indices of clinical severity of disease has been evaluated [10, 11], and MRI has been validated in comparison to alternative imaging modalities [12, 13] and correlated with histology [13, 14].

Diffusion-weighted MRI (DWI) was first employed in neuroradiological imaging of acute stroke. DWI visualizes inflammatory bowel lesions in adult patients with Crohn disease based on altered diffusivity of extracellular water in inflamed bowel wall tissue without the need for intravenous (i.v.) administration of contrast medium [15, 16]. In a previous study in adults with Crohn disease, DWI showed diagnostic performance comparable to that of T1-weighted contrast-enhanced MRI (CE-MRI) [17]. Only a limited number of studies of MRI in paediatric patients with Crohn disease is available [18–20], while there are no published data on DWI in paediatric patients with Crohn disease. DWI appears particularly suitable for MR imaging in children because of rapid image acquisition with echo-planar imaging (EPI), which allows scanning in free-breathing mode with a minimum of bulk motion artefacts, and its inherent high tissue contrast without i.v. administration of gadolinium-containing contrast medium. In contrast, abdominal MR scanning with contrast-enhanced T1-weighted sequences requires multiple cycles of breath-hold or navigator techniques and is prone to motion artefacts, particularly in young patients in a poor clinical condition. Therefore, the aim of this retrospective study was to evaluate the detectability of inflammatory bowel lesions and of extraluminal complications with DWI, compared to CE-MRI, in children and young adults with Crohn disease.

Materials and methods

Patients

We retrospectively evaluated 33 consecutive children, adolescents and young adults with confirmed Crohn disease (median age 18 years, range 10–20 years, 12 patients age ≤ 16 years) who had undergone routine small-bowel (SB) MRI with standard sequences and with DWI at our institution during a 3-year period. All study work was conducted in accordance with the Helsinki Declaration. Studies based on retrospective analysis of data from routine examinations do not require institutional review board approval at our institution. The treatment contract between patients and our university hospital covers the use of anonymized data for scientific purposes. Informed written consent was obtained from the legal guardians of all patients for all diagnostic and therapeutic measures.

The 33 children and young adults with Crohn disease underwent SB MRI because of nonconclusive preceding US

imaging or because of a discrepancy between US findings and their clinical condition (11 patients), for suspected interenteric abscess or fistula (9 patients), prior to the start of, and for therapy surveillance with, anti-TNF- α treatment (8 patients) and upon referral by external institutions (5 patients). Ten children and adolescents were newly diagnosed with Crohn disease, and nine of these (90%) had concurrent colonoscopy at our institution. None of the newly diagnosed children and young adults with Crohn disease had been treated with anti-inflammatory or steroid medication prior to MRI. Twenty-three children and young adults with previously diagnosed Crohn disease showed a median course of disease of 65 months (range 3 months to 140 months) and received anti-inflammatory, corticosteroid and/or anti-TNF- α treatment (21 patients) or were treated by the referring physician with traditional Chinese medicine alone (2 patients). In these 23 patients, concurrent colonoscopy was available in only 12, while another patient underwent ileocaecal resection 4 days after MRI. In six patients with one or more follow-up MRI examinations, only one imaging study was included.

As control, we included 27 consecutive children, adolescents and young adults (median age 16 years, range 7–20 years, 15 children age ≤ 16 years) imaged over the same period according to the same imaging protocol. These patients had been referred for MR imaging for subacute or chronic abdominal discomfort, pain and/or chronic diarrhoea (21 patients), for follow-up in Peutz-Jeghers syndrome (2 patients) and familial adenomatous polyposis (2 patients) and for oncological follow-up in tumour-free patients after resection of a gastrointestinal tumour (desmoplastic round small cell tumour in 1 patient, desmoid tumour in 1 patient). Of the 27 controls, 10 (37%) had had colonoscopy within 4 weeks of the MRI examination without macroscopic or histological evidence of chronic inflammatory bowel disease. Three other patients underwent surgical exploration and appendectomy with the final diagnosis of mild chronic appendicitis within 6 weeks of the MRI examination. The remaining controls showed no signs of chronic inflammatory bowel disease on follow-up.

Leukocyte count and serum C-reactive protein (CRP) levels determined within 1 week of MRI were available in 30 of the 33 children and young adults with Crohn disease and in 21 of the 27 controls. At our institution, the normal reference range for leukocyte count is $4.5\text{--}14.5 \times 10^3/\mu\text{l}$ in those aged 7–12 years, $4.5\text{--}13 \times 10^3/\mu\text{l}$ in those aged 13–17 years and $5\text{--}10 \times 10^3/\mu\text{l}$ in adults. The normal reference range for CRP is 0–0.5 mg/dl. Clinical disease activity in children and young adults with Crohn disease at the time of MRI examination was assessed as 1 (clinical remission or mild symptoms), 2 (moderate symptoms) or 3 (severe disease activity) based on clinical information provided by the referring clinician. Clinical data available on retrospective

analysis did not allow calculation of disease activity scores, such as the Paediatric Crohn Disease Activity Index.

MR imaging

No special patient preparation other than a 4-h fast without intake of solid foods was requested prior to MRI. Depending on age, body weight and clinical condition of the patient, 200–2,000 ml of 2.5% mannitol solution were administered as oral contrast medium over 2 h prior to imaging in all patients and controls, except in one young adult with acute abdominal discomfort who underwent emergency MRI according to the SB protocol, and did not receive oral contrast medium. The median amount of oral contrast medium administered was 1,500 ml. Two children with Crohn disease and three control patients accepted only 200–500 ml of oral contrast medium. One young adult with Crohn disease with a height of 184 cm and weight of 90 kg received 2,000 ml mannitol orally. We did not administer rectal contrast agent. All patients, except one who received an emergency scan, and all controls were given a weight-adapted dose of 20–40 mg butylscopolamine (Buscopan) i.v. for gastrointestinal hypotonia. The i.v. contrast media administered were 0.1 mmol/kg gadopentetate dimeglumine (Magnograf; Marograstr, Jena, Germany) in children and adolescents and 0.1 mmol/kg gadobutrol (Gadovist; Bayer Schering, Germany) in adults.

All MR examinations were performed in a supine position on a 1.5-T scanner (Magnetom Symphony in 20 patients, Magnetom Avanto in 40 patients; Siemens Healthcare, Erlangen, Germany) with multichannel phased-array body coils. The standard imaging protocol was performed with the breath-hold technique, and included coronal and transverse T2-weighted half-Fourier acquisition single-shot (SS) turbo spin-echo (HASTE) sequence, a coronal T1-weighted 2-D fast low angle shot (FLASH) precontrast sequence, and a transverse T1-weighted 3-D FLASH precontrast sequence, 1 min and 2 min after injection with fat saturation, as well as a contrast-enhanced transverse T1-weighted 2-D FLASH sequence and a coronal T1-weighted 3-D FLASH sequence with fat saturation. Prior to i.v. administration of contrast medium, we performed transverse free-breathing diffusion-weighted (DW) SS EPI (SS-EPI) with diffusion-sensitizing gradients applied sequentially along the three orthogonal directions.

The examination protocol implemented on the 1.5-T Magnetom Avanto scanner included the following parameters: a transverse T2-weighted HASTE sequence (TR 1,000 ms, TE 97 ms, flip angle 160°, generalized autocalibrating partially parallel acquisitions, GRAPPA, acceleration factor 2, slice thickness 8 mm, FOV 330 mm, voxel size 1.4×1.4×8 mm), a transverse DW SS-EPI sequence (TR 5,800 ms, TE 89 ms, flip angle 90°, b-values 50 and

800 s/mm², GRAPPA acceleration factor 2, epi factor 128, fat saturation, eight averages, slice thickness 6 mm, FOV 360 mm, voxel size 2.0×2.0×6.0 mm, scanning duration 4 min 56 s for 40 slices), a transverse T1-weighted 3-D FLASH sequence (TR 5.15 ms, TE 2.33 ms, flip angle 10°, GRAPPA acceleration factor 2, fat saturation, slice thickness 4 mm, FOV 330 mm, voxel size 1.9×1.0×4 mm), a transverse T1-weighted 2-D FLASH sequence (TR 110 ms, TE 4.76 ms, flip angle 90°, fat saturation, slice thickness 8 mm, FOV 330 mm, voxel size 1.5×1.0×8 mm), and a coronal T1-weighted 3-D FLASH sequence (TR 4.27 ms, TE 1.49 ms, flip angle 12°, GRAPPA acceleration factor 2, fat saturation, slice thickness 3 mm, FOV 450 mm, voxel size 2.3×1.4×3 mm).

The corresponding scan parameters for the 1.5-T Magnetom Symphony scanner were: a transverse T2-weighted HASTE sequence (TR 800 ms, TE 97 ms, flip angle 120°, slice thickness 6 mm, FOV 300 mm, voxel size 1.3×1.2×6 mm), a transverse DW-SS-EPI sequence (TR 9,000 ms, TE 126 ms, flip angle 90°, b-values 50 and 800 s/mm², epi factor 128, fat saturation, eight averages, slice thickness 6 mm, FOV 360 mm, voxel size 2.8×2.8×6.0 mm, scanning duration 7 min 21 s for 40 slices), a transverse T1-weighted 3-D FLASH sequence (TR 5.67 ms, TE 2.78 ms, flip angle 10°, fat saturation, slice thickness 5 mm, FOV 300 mm, voxel size 1.9×1.2×5 mm), a transverse T1-weighted 2-D FLASH (TR 179 ms, TE 4.75 ms, flip angle 90°, fat saturation, slice thickness 6 mm, FOV 340 mm, voxel size 1.9×1.3×6 mm), and a coronal T1-weighted 2-D FLASH sequence (TR 110 ms, TE 4.76 ms, flip angle 90°, fat saturation, slice thickness 6 mm, FOV 400 mm, voxel size 1.8×1.3×6 mm).

Image analysis

Lesions were detected by two observers in consensus. The first observer had 12 years' experience in abdominal MRI and SB MRI and 8 years' experience in paediatric MRI. The second observer had 6 years' experience in abdominal MRI and SB MRI, 4 years' experience in extraneurological DWI and 3 years' training in paediatric radiology. All quantitative image analyses were conducted by the second observer, blinded to the clinical information.

All image analyses were performed off-line on a Syngo Plaza workstation (Siemens Healthcare, Erlangen, Germany). First, the degree of bowel distension from oral contrast agent was assessed for SB and large bowel (LB) as 1 (most bowel segments collapsed), 2 (more bowel segments distended than collapsed) or 3 (nearly all bowel segments distended). The presence of inflammatory wall lesions was assessed on DW images and on CE-MR images based on criteria proposed by Alexopoulou et al. [20]. A wall thickness of >3 mm in distended bowel loops in the presence of a signal increase on DW

images and contrast enhancement was considered pathological. The presence of inflammatory bowel segments was assessed separately in the SB, the (neo-)terminal ileum, the ileocaecal junction, the caecum, the ascending, transverse and descending colon, and the rectosigmoid. The presence of abscess, fistula, stenotic bowel segment, inflammatory conglomerate, skip lesions of the SB, comb sign and regional lymphadenopathy was also recorded. One affected SB segment and one affected LB segment (where inflammatory signal alterations were most prominent) were analysed quantitatively per patient, in comparison to adjacent normal-appearing bowel segments.

The degree of distension was assessed and wall thickness, the signal intensity of the bowel and bowel lumen were measured, together with the standard deviation of image noise on corresponding transverse DW images with $b=800$ s/mm² and T1-weighted CE-MR images. Total apparent diffusion coefficient (ADC_{total} , $50/800$) was measured on automatically generated ADC maps. Three small circular regions of interest (ROIs) with a diameter equivalent to the thickness of the intestinal wall were placed on each assessed bowel segment (Fig. 1) and the mean values were recorded for statistical analysis. The mean ROI area was 3.2 ± 0.7 mm² (mean \pm standard deviation) in normal SB segments, 3.2 ± 0.8 mm² in normal LB segments, 25.2 ± 14.3 mm² in inflamed SB and 21.4 ± 9.0 mm² in inflamed LB.

Signal intensity (SI) ratios for SB and LB segments, calculated as $(SI_{inflamed}/SI_{normal})$ and as $(SI_{inflamed} - SI_{normal})$ divided by the standard deviation of the background noise, were used for signal quantification. In addition, ADC values measured in muscle (erector spinae), liver, spleen and renal cortex and the fluid signal of the urinary bladder, the renal pelvis and the cerebrospinal fluid were used as internal reference standards. Images were fused off-line using dedicated 3-D image fusion software (Siemens Healthcare, Erlangen Germany) on the scanner workstation.

Intraobserver variability was determined by means of a second blinded measurement in ten randomly chosen datasets. The coefficient of variation (CV, standard deviation divided by the mean) was calculated as 9.4% for normal bowel wall, 7.9% for inflamed bowel segments and 16.2% for ADC of inflamed bowel wall.

Statistical analysis

Normally distributed data are presented as means \pm standard deviation. Frequency proportions were analysed with the chi-squared test and Fisher exact test on crosstabs. Groups were compared with the independent sample *t*-test for normally distributed variables and with the Mann-Whitney test for variables deviating from a normal distribution. For between-group comparison of related variables, we employed the nonparametric Wilcoxon signed rank test. The associations between

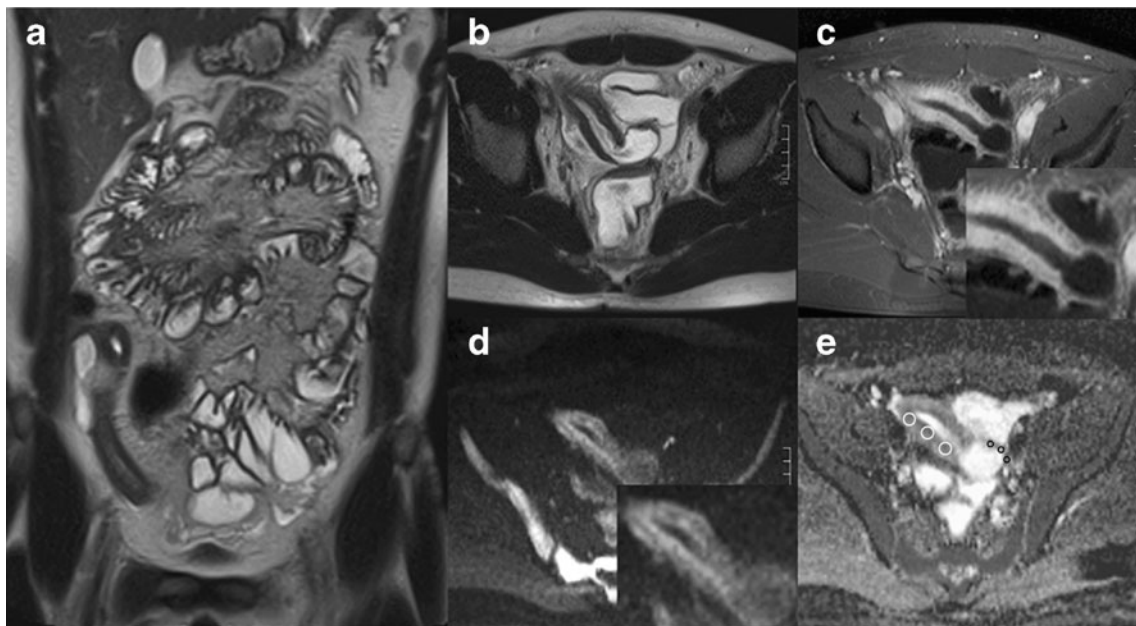


Fig. 1 Newly diagnosed Crohn disease in a male patient with reduced physical fitness for 1 month. The patient did not report abdominal pain, fever or diarrhoea. leukocyte count was $5.5 \times 10^3/\mu\text{l}$, and serum CRP was elevated (2.35 mg/dl). Coronal and transverse T2-weighted HASTE images (**a**, **b**) show marked segmental wall thickening of the terminal ileum, and the corresponding two-layered signal increase on

the T1-weighted CE-MR image (**c**) and the $b=800$ DW image (**d**) indicate concurrent transmural inflammation and severe mucositis. **e** ADCs were calculated from the average of three small circular ROIs as 0.84×10^{-3} mm²/s for inflamed SB (white ROIs) and 1.77×10^{-3} mm²/s for adjacent normal SB (black ROIs)

continuous variables were evaluated with Pearson’s bivariate correlation analysis. All statistical tests were performed two-sided at the level of $P < 0.05$. Analyses were performed with the IBM SPSS Statistics 20 software package for Windows.

Results

The patient group and the control group were matched in terms of gender composition and distribution between the two MRI scanners (Table 1). The mean ages of patients with newly diagnosed disease and those with known Crohn disease did not differ significantly (16.7 ± 3.9 vs. 17.3 ± 2.8 years; independent sample t -test, $P = 0.599$). The latter reported a mean age at first diagnosis of 11.9 ± 4.9 years (range 5–19 years).

Qualitative analysis

All imaging studies in patients and controls yielded images of diagnostic quality. Contrast-enhanced T1-weighted sequences showed moderate motion artefacts in six examinations, while four DWI studies suffered from mild to moderate distortion artefacts. Among all 33 patients, DWI and CE-MRI correctly identified the Crohn disease in 32 and 31, respectively (Table 2). No false-positive results occurred in controls. The terminal ileum and the ileocaecal junction was the most commonly observed manifestation of Crohn disease (Fig. 1). DWI showed active segmental inflammation of the small intestine with wall thickening of >3 mm and corresponding signal increases at high b-values in 22 of the 33 patients with Crohn disease. On CE-MRI, one of these patients was judged as normal, while active inflammation of the terminal ileum was confirmed by endoscopy. The majority of children and young

Table 1 Characteristics of the study cohort and MRI examinations. The numbers of subjects of each gender and scanned with each MRI scanner, and the degrees of bowel distension were evaluated with the chi-square test, and differences in mean age with the Mann-Whitney test

	Patients	Control	<i>P</i> value
No. of subjects	33	27	
Gender female/male (<i>n</i>)	18/15	18/9	0.340
Age (years)	17 ± 3	15 ± 4	0.034
MRI scanner Avanto/Symphony (<i>n</i>)	24/9	16/11	0.271
Artefacts (<i>n</i>)			
DWI	1	3	
T1-weighted CE-MRI	4	2	
Degree of bowel distension, 1/2/3 (<i>n</i>)			
Small bowel	2/21/10	3/14/10	0.603
Large bowel	7/19/7	4/12/11	0.257

Table 2 MRI findings in 33 children and young patients with Crohn disease based on a per-patient analysis of DW and CE-MR images. CE-MRI was the only reference standard for SB lesions. For terminal ileal and colonic lesions, endoscopy was used as the reference if available, while CE-MRI was used as the reference in the remaining patients. The Wilcoxon signed rank test was used to compare wall thickness and signal intensity measured on CE-MR and DW images. The signal intensity (SI) ratio of inflammatory contrast enhancement was calculated as $(SI_{\text{inflamed}} - SI_{\text{normal}})$ divided by the standard deviation of the noise

	Reference	CE-MR images	DW images	<i>p</i> value
True-positive patients with Crohn disease (<i>n</i>)	33	31	32	
Inflammatory wall lesions (<i>n</i>)				
Small bowel	4	4	4	
Terminal ileum and ileocaecal junction	22	21	22	
Colon	19	16	18	
Rectosigmoid	14	12	14	
False-positive findings (<i>n</i>)				
Small bowel		0	0	
Large bowel		1	2	
Crohn complications (<i>n</i>)				
Abscess		3	3	
Stenosis		3	3	
Fistula		1	1	
Inflammatory conglomerate		1	1	
Small bowel skip lesion		6	6	
Comb sign		15	8	
Lymphadenopathy		14	23	
Small-bowel wall thickness (mean \pm SD, mm)				
Normal distended segment		1.9 ± 0.2	2.2 ± 0.2	<0.001
Inflamed segment		5.4 ± 1.6	5.5 ± 1.4	0.303
Large bowel wall thickness (mean \pm SD, mm)				
Normal distended segment		1.8 ± 0.2	2.2 ± 0.2	<0.001
Inflamed segment		5.2 ± 1.1	5.2 ± 1.2	0.791
Signal intensity ratio for inflamed bowel wall (mean \pm SD)				
Small bowel		41.6 ± 29.6	29.5 ± 17.5	0.144
Large bowel		56.6 ± 34.1	34.4 ± 24.4	0.015

adults with inflammatory LB lesions were correctly identified (Table 2). One 10-year-old boy with newly diagnosed Crohn disease and mild segmental colitis in the ascending colon on colonoscopy did not show any suspicious signal alterations or wall thickening either on DWI or on CE-MRI, although paracolic regional lymphadenopathy was observable on DWI as an indirect sign of inflammation. In two other children with inflammatory colonic and rectosigmoid wall lesions, T1-weighted CE-MRI produced a false-negative finding as a result

of susceptibility artefacts from intraluminal gas within the affected bowel segment. Both CE-MRI and DWI gave false-positive results in collapsed colon segments: wall-thickening on T2-weighted HASTE images and signal increases on DWI and T1-weighted CE-MRI wrongly suggested inflammation (Table 2). As these false-positive findings all occurred in children and young adults with additional true-positive SB or LB segments, the diagnostic performance shown in the per-patient analysis was not adversely affected. Overall diagnostic accuracy for identifying children and young adults with inflammatory bowel lesions among patients and controls was 59/60 (98%) for DWI and 58/60 (97%) for CE-MRI.

Crohn complications were seen in 6 of 33 children and young adults with Crohn disease (18%) and were consistently diagnosed by both DWI and contrast-enhanced sequences (Table 2, Fig. 2). Abscess formations were correctly identified in three adolescents and young adults. However, the characteristic high signal intensity of purulent fluid on $b=800$ DW images (Fig. 2) and the low mean ADC facilitated more rapid detection on DW images than on T1-weighted CE-MR images. The mean ADC of abscess was $0.73 \times 10^{-3} \text{ mm}^2/\text{s}$. Relevant intestinal obstruction was seen in three children and young adults with Crohn disease with SB dilatation proximal to inflamed segments. Six SB skip lesions were all correctly identified on both DW images and CE-MR images.

Regional lymphadenopathy was shown as present in 23 children and young adults with Crohn disease on DWI, but only in 14 of these 23 patients on CE-MRI. The comb sign, indicating increased mesenteric blood supply to inflamed bowel segments, was observed in 15 children and young adults with Crohn disease on CE-MRI. DWI at high b-values did not show corresponding signal alterations, while DWI at low b-values showed a radial mesenteric signal increase adjacent to affected segments in 8 of these 15 patients.

Quantitative analysis

The maximum measured thicknesses of normal distended SB and LB wall were 2.3 mm and 2.5 mm on T2-weighted HASTE images, 2.5 mm and 2.6 mm on DW images and 2.3 mm and 2.4 mm on CE-MR images, respectively. The mean measured wall thicknesses of noninflamed bowel segments were higher on DW images than on CE-MR images ($2.2 \pm 0.2 \text{ mm}$ vs. $1.9 \pm 0.2 \text{ mm}$; $P < 0.001$, Wilcoxon signed rank test). No significant differences in mean wall thickness between children with Crohn disease and controls were seen in noninflamed and distended SB and LB segments.

Inflamed bowel segments were characterized by significant wall thickening with minimum/average/maximum wall thicknesses of 3.6/5.4/8.8 mm on T2-weighted HASTE

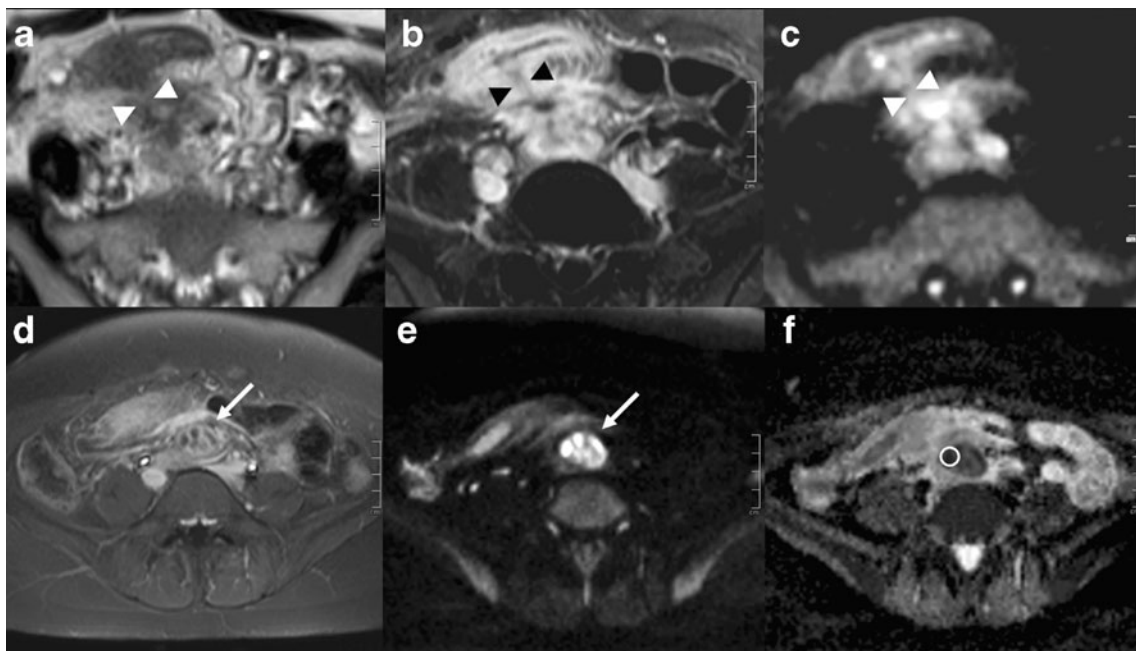


Fig. 2 Primary manifestation of Crohn disease in a young woman with acute abdominal pain, fever and malaise for 2 weeks. In addition to terminal ileitis and an ileal skip lesion, MRI showed an inflammatory conglomerate with interenteric fistulae and fistulous penetration into the mesenteric root, confirmed on surgical resection and histopathology. **a–c** The T2-weighted HASTE image (**a**) and the $b=800$ DW image (**c**) show the inflammatory bowel lesions and a fistula (*arrowheads*); the T1-weighted CE-MR image (**b**) provides superior spatial

resolution. Note the two-layered signal of the SB wall on the T1-weighted CE-MR image and the DW image, and the comb sign on the T1-weighted CE-MR image. **d, e** The T1-weighted CE-MR image (**d**) and the $b=800$ DW image (**e**) show a mesenteric abscess on adjacent cross-sections (*arrows*), which is more readily detectable on the DW image. **f** Mean ADC was measured as $0.61 \times 10^{-3} \text{ mm}^2/\text{s}$ with a small ROI placed on the abscess cavity

images, 3.5/5.5/8.3 mm on DW images and 3.1/5.4/9.0 mm on CE-MR images for SB lesions, and 3.1/4.9/6.5 mm on T2-weighted HASTE images, 3.9/5.2/7.6 mm on DW images and 3.6/5.2/7.2 mm on CE-MR images for LB lesions. Mean wall thickness did not show significant differences between DW and CE-MR images for inflamed SB (5.5±1.4 mm vs. 5.4±1.6 mm; $P=0.303$, Wilcoxon signed ranks test) or LB (5.2±1.2 mm vs. 5.2±1.1 mm; $P=0.791$, Wilcoxon signed rank test) segments. The signal intensity of inflamed segments was significantly higher than that of normal segments on both b=800 DW images and on CE-MR images. Mean signal intensity ratio of inflamed to normal bowel wall was 3.8 (range 2.1 to 5.7) on b=800 DW images and 4.2 (range 1.9 to 9.2) on CE-MR images in SB lesions and 4.9 (range 2.6 to 9) on b=800 DW images and 3.6 (range 1.6 to 6.9) on CE-MR images in LB lesions. Mean signal intensity ratio ($SI_{inflamed} - SI_{normal}$) divided by the standard deviation of the noise was higher for CE-MR images than for DW images ($P=0.015$, Wilcoxon signed rank test; Table 2). In contrast, the detectability of inflammatory SB wall lesions within the surrounding tissue by DWI was superior in 8 of 24 lesions (33%) and equal to T1-weighted CE-MRI in 15 of 24 lesions (63%), while one lesion only was more easily identified on T1-weighted CE-MRI. In 21 LB lesions, DWI was considered superior to T1-weighted CE-MRI in four patients (19%) and equal in the remaining patients.

In inflamed bowel wall, two patterns of signal alteration were discernible: a transmural homogeneous signal increase and a layered pattern with a marked signal increase in the inner layer and a less pronounced signal increase in the peripheral layer (Figs. 1 and 2). Of 24 SB lesions, 7 (29%) showed layered signal changes on DW images and, among these, 3 lesions were seen with layered contrast enhancement on CE-MR images. Of 21 LB lesions, 7 (33%) showed such a pattern on DW images, with four of these lesions also exhibiting layered contrast enhancement on T1-weighted MR images. One LB lesion had a layered pattern on CE-MR images only. A layered pattern was observed in 1 of 10 children and young adults with newly diagnosed Crohn disease (10%) and in 10 of 23 children and young adults with known Crohn disease (43%; $P=0.061$, Fisher exact test).

Compared to normal bowel segments, inflamed segments showed markedly restricted diffusion with high signal on b=800 DW images and with low ADC, virtually without overlap with normal bowel wall (Table 3). Bivariate correlation indicated a significant inverse correlation between wall thickness and ADC in inflamed segments (Pearson's $r=-0.39$, $P=0.008$), but not in normal segments (Pearson's $r=0.04$, $P=0.671$). On T1-weighted CE-MR images, increased signal in inflamed bowel segments did not correlate with corresponding wall thickness (Pearson's $r=0.01$, $P=0.975$). No correlation was observed between ADC and contrast enhancement of inflamed bowel segments.

Table 3 ADC_{total} 50/800 in various organs, body fluids and normal distended bowel wall in patients and controls and in inflamed bowel wall in patients

	ADC (10 ⁻³ mm ² /s)	
	Mean	Range
Internal reference (patients and controls)		
Muscle	1.22±0.09	1.03–1.41
Liver	1.10±0.08	0.92–1.32
Spleen	0.84±0.08	0.65–1.02
Kidney	1.85±0.09	1.65–2.07
Renal pelvis	3.21±0.43	2.26–4.28
CSF	3.35±0.30	2.89–4.29
Urinary bladder	3.17±0.38	2.51–4.08
Normal distended bowel wall (patients and controls)		
Small bowel	2.08±0.16	1.77–2.44
Large bowel	2.01±0.14	1.61–2.24
Inflamed bowel wall (patients only)		
Small bowel	1.16±0.18	0.84–1.40
Large bowel	1.21±0.21	0.84–1.60

Children and young adults with Crohn disease had a higher leukocyte count and higher serum CRP ($P=0.041$ and $P<0.001$, respectively; Mann-Whitney test) in the presence of severe clinical symptoms, compared to other patients and controls. Contrast enhancement of inflamed bowel wall showed a strong correlation with leukocyte count (Pearson's $r=0.67$, $P=0.001$) and CRP (Pearson's $r=0.57$, $P=0.008$) in SB lesions, and with CRP (Pearson's $r=0.49$, $P=0.036$) in LB lesions. Correlation analysis of ADC values in inflamed SB and LB segments did not show statistically a significant association with severity of clinical symptoms, nor with laboratory markers or contrast enhancement.

Discussion

A significant percentage of patients with Crohn disease are first diagnosed during childhood and adolescence [1]. The chronic course of disease with alternating states of remission and recurrence, compromising quality of life and physical development of the affected young patients, the need for therapy surveillance and the dilemma of how to time surgical intervention necessitate frequent diagnostic imaging studies. In CT and with conventional enteroclysis, high doses of ionizing radiation accumulate over the course of the disease [4, 5, 21]. US is widely employed as the first-line imaging modality in children for screening in chronic inflammatory bowel disease, for evaluation of extent and disease activity and for therapy surveillance [6]. MRI is increasingly considered the imaging modality of choice for further diagnostic workup if US imaging remains inconclusive or fails to provide all therapeutically relevant

information [9, 22]. State-of-the-art MRI protocols usually require administration of oral and i.v. contrast medium, and use T2-weighted sequences with and without fat saturation as well as contrast-enhanced T1-weighted sequences with 2-D and/or 3-D acquisitions and breath-hold techniques [9]. In recent years, DWI has been introduced as a new sequence for abdominal MRI. DWI has shown very promising results in a the small number of published studies in patients with chronic inflammatory bowel disease available so far [15, 16]. A recent study evaluated the feasibility of DWI in a large cohort of adult patients with chronic inflammatory bowel disease and showed a high accuracy of DWI for detection of inflammatory lesions, as compared to colonoscopy, without the need of bowel preparation and without oral or rectal administration of contrast medium [23]. Paediatric patients, who are most eligible for MRI as a radiation-free imaging modality, also pose a particular challenge, as patient compliance is often limited with regard to breath-hold techniques, avoidance of patient movement during image acquisition, long scan times and i.v. injections. We therefore sought to evaluate DWI not as an adjunct, but as an alternative to standard CE-MRI protocols in a cohort of children, adolescents and young adults with Crohn disease.

Comparison of DWI and CE-MRI

An important finding of our study was that free-breathing DW SS-EPI as a stand-alone technique in combination with T2-weighted HASTE demonstrates diagnostic performance equal, if not superior, to CE-MRI for detecting SB and LB lesions, as well as extraluminal complications in children and young adults with Crohn disease, as compared to matched controls. Both imaging approaches yielded high diagnostic accuracy, especially in SB lesions. However, DWI showed better detectability of inflammatory lesions, as based on subjective judgement. The high b-value of 800 s/mm^2 we used facilitates strong suppression of background signal arising from noninflamed tissue and from body fluids, so that inflamed bowel segments stand out from, and are more easily detected within, surrounding anatomical structures. In routine imaging, this might be particularly advantageous for less experienced readers. Future studies may address the interesting question as to whether there are different learning curves for DWI and CE-MRI. However, DWI still has a relatively low spatial resolution (2.0×2.0 to 2.8×2.8 mm in-plane in our study). DWI should therefore be evaluated in combination with a high-resolution standard MRI sequence. We chose T2-weighted HASTE for its fast image acquisition and its bright fluid signal. Based on these two sequences, comprehensive diagnostic imaging without a substantial loss of diagnostic information and without the need of i.v. administration of contrast medium seems feasible with a scan time of less than 10 min per patient. If possible, depending on patient

condition, a standard MRI sequence with high spatial resolution, e.g. T2 TSE, contrast-enhanced T1-weighted imaging with or without fat saturation or a high-resolution T1-weighted 3-D water excitation “fistula sequence”, should also be acquired, particularly in patients with a suspected interenteric, mesenteric or pelvic floor fistula.

Apart from the limited spatial resolution of DWI, the presence of image artefacts is another issue of concern. The DW sequence employed in our study was based on SS-EPI. Ultrafast imaging acquisition with EPI and with multiple averages renders the sequence relatively insensitive to bulk motion with virtually no motion artefacts in free-breathing mode. Contrast-enhanced sequences acquired in breath-hold mode, on the other hand, are prone to motion artefacts from insufficient breath-hold, which was most pronounced in the dynamic T1-weighted 3-D FLASH study. Susceptibility to artefacts is an important technical disadvantage of DWI based on SS-EPI. Primary acquisition of coronal or sagittal cross-sections usually results in severe distortion artefacts and non-diagnostic image quality secondary to B0 magnetic field inhomogeneity. Transverse acquisition in DWI with secondary multiplanar reconstruction (MPR) avoids this issue; however, image quality then depends on the use of thin axial slices. Figure 3 presents an example from our study cohort showing compromised image quality in DWI with a 6-mm transverse slice thickness on coronal reconstruction, in comparison to a coronal contrast-enhanced T1-weighted image, while all relevant diagnostic information is retained in the DW reconstruction. In our study, DWI and contrast-enhanced sequences were complementary with regard to the presence of artefacts.

Image fusion

Image fusion of standard MRI sequences with DWI is a new mode for the visual presentation of pathological findings (Figs. 3 and 4). The semitransparent overlay of coloured DW images facilitates collocation of signal changes and easier detection of lesions, comparable to PET/MRI or PET/CT image fusion techniques. Overlay of ADC maps for tissue characterization is also feasible [24]. Future software solutions should include easy-to-use options for online and offline image fusion of standard sequences with diffusion-weighted MR image sets.

Diagnostic challenges with DWI and CE-MRI

Only one patient with false-negative findings was observed in our study group. A 10-year-old boy with newly diagnosed mild Crohn colitis in the ascending colon presented with mild clinical symptoms and without laboratory markers of active inflammation. Even on retrospective analysis, no indication of inflammatory wall lesions was seen. Regional

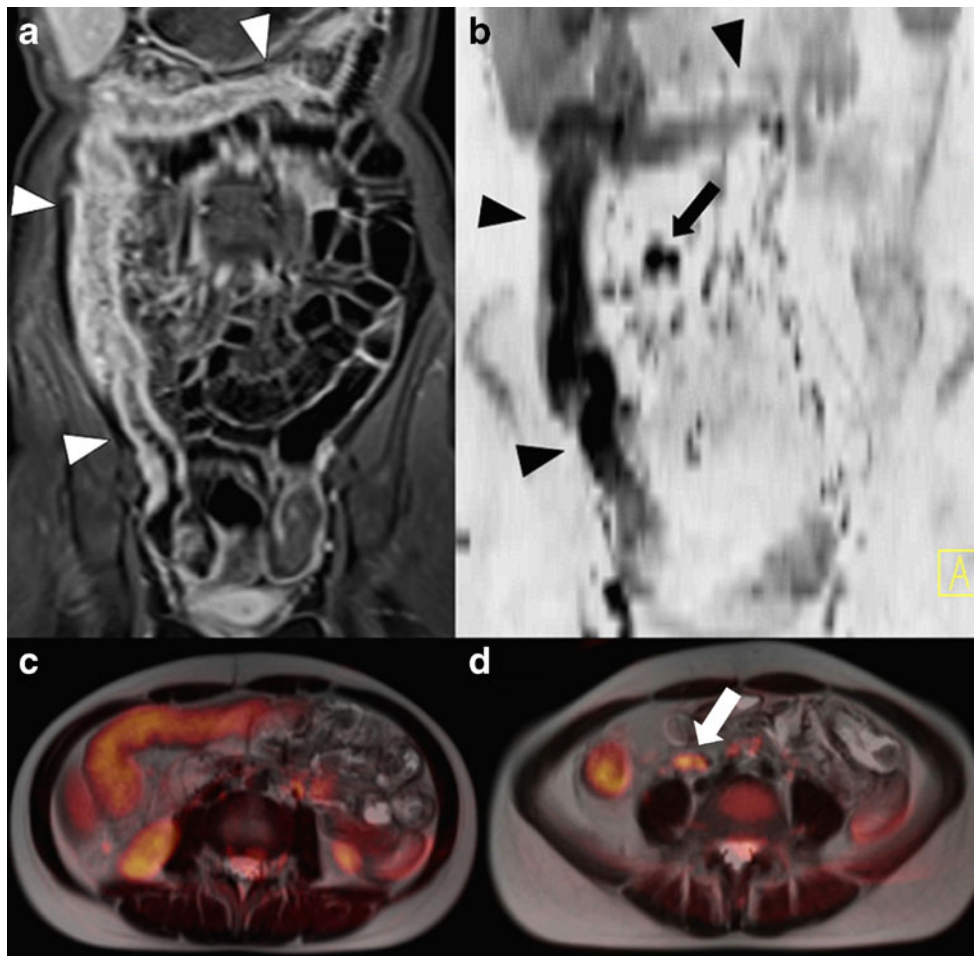


Fig. 3 Acute exacerbation of Crohn disease. **a, b** Inflammatory wall lesions involving the terminal ileum as well as the ascending and transverse colon are clearly discernible (*arrowheads*) on coronal contrast-enhanced T1-weighted images (**a** curved MPR of coronal T1-weighted 2-D FLASH acquisition with fat saturation, **b** maximum-intensity projection of $b=800$ DWI, coronal MPR of transverse DWI, inverted grey scale for visual presentation). **c, d** Fusion of transverse T2-weighted HASTE and coloured $b=800$ DW images at the level of the right colon flexure (**c**)

and the ascending colon (**d**) show inflammatory signal changes on the DW images as a coloured semitransparent overlay. The absence of inflammatory colonic wall lesions distal to the left colonic flexure was confirmed on concurrent colonoscopy. DWI visualizes inflammatory mesenteric lymphadenopathy (**b, d** *arrows*). Caudal cross-sections of the right hepatic lobe and both kidneys are shown in the DW image (**c**) with a bright coloured signal in, which is physiological

lymphadenopathy observed in this boy may be considered a nonspecific sign of occult bowel inflammation. Another patient with endoscopically confirmed focal inflammation of the descending colon showed corresponding signal changes on DWI, but not on CE-MRI. The small number of false-positive and false-negative findings observed for colon segments did not affect the overall classification of these patients. These misclassifications were caused by artefacts arising from a lack of intraluminal contrast and distension and from artefacts caused by colonic gas and stool filling. A signal increase in collapsed SB and LB segments is a common finding on both contrast-enhanced sequences [25] and on DWI. In contrast to the conclusion drawn from one earlier study [23], we consider administration of a sufficient amount of oral contrast medium necessary to maintain high diagnostic specificity. Rectal administration of contrast medium may be a helpful option in those

patients who are not scheduled for concurrent colonoscopy and in whom evaluation of colonic segments with high diagnostic confidence is important for diagnosis and treatment.

Differentiation of acute and chronic inflammation

The morphological characteristics of inflamed bowel loops on CE-MRI have previously been described as homogeneous slow enhancement in inactive chronic Crohn disease and as layered with strong, rapid mucosal contrast enhancement in active disease [26]. In our study, the predominant morphological pattern in 90% of patients with newly diagnosed Crohn disease was that of homogeneous transmural inflammation on T1-weighted CE-MRI and on DWI, while nearly one-half of children and young adults with known, and treated, Crohn disease showed a layered pattern of

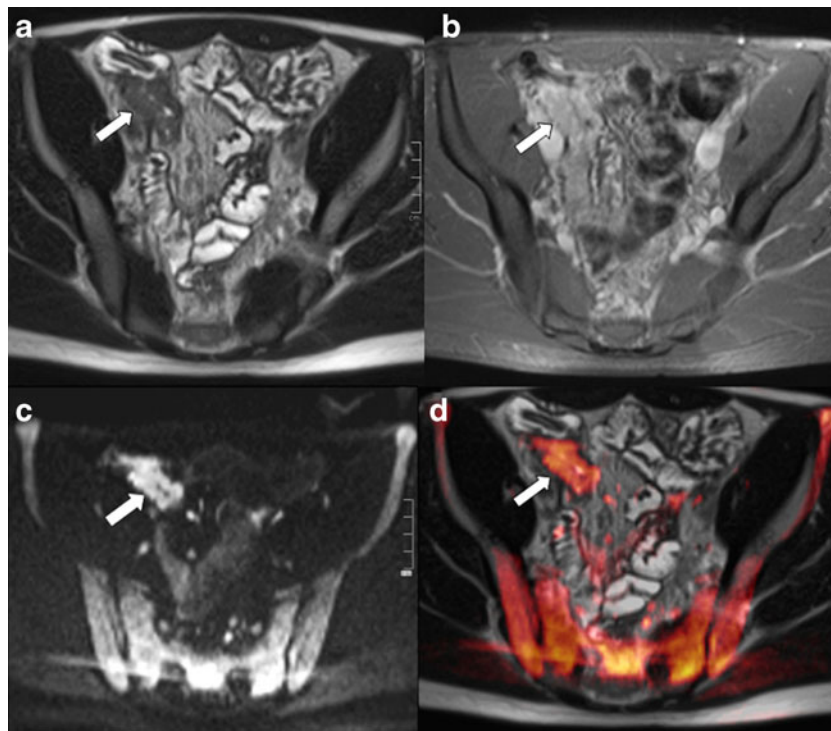


Fig. 4 Segmental inflammatory wall lesion in the terminal ileum in a 20-year-old patient who had been diagnosed with Crohn disease 9 months previously and reported moderate clinical symptoms with abdominal pain and increased stool frequency at the time of examination. The lesion (arrows) is delineated on corresponding transverse cross-sections of T2-weighted HASTE (a), contrast-enhanced T1 2-D FLASH with fat saturation (b), b:800 DWI (c) acquisitions and on the fused image from

transverse T2-weighted HASTE and coloured b=800 DWI (d). High signal intensity of pelvic bone marrow on DWI (as seen in d) is common in children and in patients with increased haematopoiesis, but is also frequently seen in young adults with Crohn disease (compare Fig. 1), hypothetically secondary to bone marrow stimulation by inflammatory stimuli or by gastrointestinal bleeding

contrast enhancement. Layered wall morphology has been attributed to exacerbation of mucosal inflammation in chronic disease [26]. A modifying effect of antiinflammatory medication on contrast-enhancement dynamics and on ADC can be assumed. The morphological pattern may indicate different stages of disease activity and therapy response and would thus be of practical significance. However, a layered signal pattern was not entirely consistent for CE-MRI and DWI. DWI appears more sensitive for detecting layered wall signal, as compared to CE-MRI. Further investigations are necessary to verify the typical morphological patterns of signal changes in acute and chronic disease.

Attempts to correlate clinical disease activity with dynamic contrast enhancement of inflamed bowel wall on MRI have not produced conclusive answers so far [11]. Although an association with disease activity can be assumed in general, previous studies with meticulous image analysis of the contrast enhancement in affected bowel segments and its correlation with Crohn activity scores have shown equivocal findings with no [20], weak to moderate [26, 27] and strong correlations [28]. In our study group, we observed significantly elevated leukocyte count and serum CRP in patients with severe symptoms. CRP and leukocyte count showed moderate associations with segmental contrast enhancement in children

and adults with Crohn disease. Otherwise, the clinical data available for our retrospective analysis were not sufficient to calculate clinical disease activity scores and a comprehensive analysis in this respect was beyond the scope of this study.

As in previous reports, ADC as a quantitative measure of diffusivity indicated markedly restricted diffusion within inflamed bowel wall with mean values around $1.2 \times 10^{-3} \text{ mm}^2/\text{s}$ in our study. Mean ADC values for inflamed and normal bowel wall were lower in our study, compared with data presented by Kiryu et al. [15], but fall within the range of ADC reported by Oto et al. [16]. Oussalah et al. [23] used DWI for lesion detection, but did not measure ADC. ADC values are to some extent influenced by the scanning parameters, particularly by the technical specifications of the DW sequence and the b-values used for image acquisition. Study data reporting ADC values should therefore include reference values for body tissues and fluids to facilitate comparability between different examination protocols. The ADC measured for inflamed bowel wall in our study did not show any significant correlation with clinical disease severity and laboratory parameters. The underlying biophysical cause of restricted diffusion within inflamed soft tissue still awaits clarification. A potential pathogenetic mechanism may include a reduction in extracellular space secondary to cell

swelling or increased cell density caused by migration of lymphocytes into the inflamed wall segments. Dynamic T1-weighted scanning should, in principle, facilitate superior quantification of local bowel inflammation and should be able to quantify response to therapy [20]. ADC as a measure of diffusivity and of bowel wall infiltration with inflammatory cells should carry the same potential, in theory. A crucial issue for clinical research in Crohn disease is the definition of valid outcome variables, as a strong intervening influence of psychological factors has to be taken into account. Further research is necessary to provide a valid multifactorial conceptual framework for future clinical evaluation of dynamic CE-MRI and quantitative ADC measurement in chronic inflammatory bowel disease.

Limitations

Major limitations of our study arise from the retrospective design. As a result of retrospective data collection, information on clinical disease activity and on US imaging was incomplete so that we could not comprehensively analyse MRI findings in correlation with clinical symptoms or with US as a potential diagnostic reference. We therefore had to limit our analysis to a comparison of the two MR imaging techniques that were central to the purpose of our study. The reference standard chosen for any imaging study in Crohn disease is an issue of concern. SB lesions are for the most part inaccessible to endoscopy. CE-MRI has been studied and validated in comparison to radiographic SB series [29] and was therefore defined as our reference standard for SB lesions. Endoscopy is the recognized reference standard for inflammatory lesions of the ileocolic junction and the LB. CE-MRI provides a moderate to high diagnostic accuracy, compared to other modalities, including colonoscopy and US [30], and to histology [31]. As colonoscopy was available in about two-thirds of the children and young adults with Crohn disease and in only one-third of controls, we used colonoscopy as the reference where available and CE-MRI in the remaining patients and controls. Ultrasonography should be employed as the reference standard in future studies of DWI in Crohn disease.

The relatively small size of the study group is another limitation of our study. As US examination is sufficient in most instances, only a relatively small number of children with Crohn disease are referred to MRI. There are no data on substantially larger paediatric patient cohorts available at present, and none of the studies available included a matched control group. A multicentre study approach with standardized examination protocols may be necessary to recruit larger patient cohorts. MRI examinations in our study were performed on two different MR scanners from the same manufacturer. Although the scanning protocols used similar examination parameters as far as possible, a possible influence

of hardware and software configuration on our study results cannot be ruled out, although the internal reference measurements did not reveal substantial differences between the scanners. Another technical issue of concern is the limited spatial resolution of MR sequences, and particularly of DWI, relative to the thickness of the intestinal wall. The 6-mm slice thickness of DWI, in particular, renders quantitative analysis of bowel wall ADC susceptible to partial volume effects. The relatively high coefficient of variation observed for mean ADC of bowel wall, compared with recently published data on ADC of parenchymatous abdominal organs [32], may have been a result of limited in-plane and through-plane resolution of the DW sequences employed in our study. Semiautomatic ROI quantification may be superior to manual ROI selection and should be evaluated in future studies. A significant reduction in slice thickness and an increase in spatial resolution, as an alternative approach, would imply substantially longer scan durations. With the scanner equipment presently available, quantitative ADC measurement of inflamed bowel wall for correlation with signal intensity of standard sequences or with clinical indicators of disease activity may therefore be of limited diagnostic value. Partial volume effects and sampling errors certainly also affect ROI measurement on standard MRI sequences.

The study presented can be considered proof-of-concept work and relied on one experienced observer for quantitative analysis. Future studies should include interobserver variability analyses and observations obtained at different levels of experience to search for differences in the learning curves with DWI and standard MRI sequences.

Conclusion

Our study provides evidence that DWI shows diagnostic accuracy comparable to that of CE-MRI and has potential as a stand-alone imaging technique for the diagnostic work-up in children and young adults with known or suspected Crohn disease. A streamlined scanning protocol including DWI in free-breathing mode and fast T2-weighted imaging is likely to result in better patient compliance, and therefore improved image quality, particularly in young patients in a poor clinical condition. On the basis of our preliminary findings, further evaluation is warranted, ideally in multicentre studies with larger patient cohorts, standardized MRI protocols and preferably a multimodal comprehensive reference standard, including US, endoscopy, clinical disease activity scores, and histology.

Acknowledgments We would like to thank our Medical Radiation Technologists Mrs. C. Doernfeld and Mrs. U. Pytlík and the MR imaging team for performing the MRI scans and for taking care of patients and parents. We also thank Dr. N. Hassold for correcting the manuscript and spell-checking.

Conflicts of interest The authors have no conflicts of interest to declare.

References

- Hyams JS (1996) Crohn's disease in children. *Pediatr Clin North Am* 43:255–277
- Loftus EV (2004) Clinical epidemiology of inflammatory bowel disease: Incidence, prevalence, and environmental influences. *Gastroenterology* 126:1504–1517
- Diefenbach KA, Breuer CK (2006) Pediatric inflammatory bowel disease. *World J Gastroenterol* 12:3204–3212
- Desmond AN, O'Regan K, Curran C et al (2008) Crohn's disease: factors associated with exposure to high levels of diagnostic radiation. *Gut* 57:1524–1529
- Peloquin JM, Pardi DS, Sandborn WJ et al (2008) Diagnostic ionizing radiation exposure in a population-based cohort of patients with inflammatory bowel disease. *Am J Gastroenterol* 103:2015–2022
- Alison M, Kheniche A, Azoulay R et al (2007) Ultrasonography of Crohn disease in children. *Pediatr Radiol* 37:1071–1082
- Semelka RC, Shoenut JP, Silverman R et al (1991) Bowel disease: prospective comparison of CT and 1.5-T pre- and postcontrast imaging with T1-weighted fat-suppressed and breath-hold FLASH sequences. *J Magn Reson Imaging* 1:625–632
- Shoenut JP, Semelka RC, Magro CM et al (1994) Comparison of magnetic resonance imaging and endoscopy in distinguishing the type and severity of inflammatory bowel disease. *J Clin Gastroenterol* 19:31–35
- Siddiki H, Fidler J (2009) MR imaging of the small bowel in Crohn's disease. *Eur J Radiol* 69:409–417
- Kettritz U, Isaacs K, Warshauer DM et al (1995) Crohn's disease. Pilot study comparing MRI of the abdomen with clinical evaluation. *J Clin Gastroenterol* 21:249–253
- Horsthuis K, Bipat S, Stokkers PCF et al (2009) Magnetic resonance imaging for evaluation of disease activity in Crohn's disease: a systematic review. *Eur Radiol* 19:1450–1460
- Horsthuis K, Lavini C, Stoker J (2005) MRI in Crohn's disease. *J Magn Reson Imaging* 22:1–12
- Gee MS, Nimkin K, Hsu M et al (2011) Prospective evaluation of MR enterography as the primary imaging modality for pediatric Crohn disease assessment. *AJR* 197:224–231
- Punwani S, Rodriguez-Justo M, Bainbridge A et al (2009) Mural inflammation in Crohn disease: location-matched histologic validation of MR imaging features. *Radiology* 252:712–720
- Kiryu S, Dodanuki K, Takao H et al (2009) Free-breathing diffusion-weighted imaging for the assessment of inflammatory activity in Crohn's disease. *J Magn Reson Imaging* 29:880–886
- Oto A, Zhu F, Kulkarni K et al (2009) Evaluation of diffusion-weighted MR imaging for detection of bowel inflammation in patients with Crohn's disease. *Acad Radiol* 16:597–603
- Oto A, Kayhan A, Williams JT et al (2011) Active Crohn's disease in the small bowel: evaluation by diffusion weighted imaging and quantitative dynamic contrast enhanced MR imaging. *J Magn Reson Imaging* 33:615–624
- Laghi A, Borrelli O, Paolantonio P et al (2003) Contrast enhanced magnetic resonance imaging of the terminal ileum in children with Crohn's disease. *Gut* 52:393–397
- Toma P, Granata C, Magnano G et al (2007) CT and MRI of paediatric Crohn disease. *Pediatr Radiol* 37:1083–1092
- Alexopoulou E, Roma E, Loggitsi D et al (2009) Magnetic resonance imaging of the small bowel in children with idiopathic inflammatory bowel disease: evaluation of disease activity. *Pediatr Radiol* 39:791–797
- Sauer CG, Kugathasan S, Martin DR et al (2011) Medical radiation exposure in children with inflammatory bowel disease estimates high cumulative doses. *Inflamm Bowel Dis* 17:2326–2332
- Wiarda BM, Kuipers EJ, Houdijk LP et al (2005) MR enteroclysis: imaging technique of choice in diagnosis of small bowel diseases. *Dig Dis Sci* 50:1036–1040
- Oussalah A, Laurent V, Bruot O et al (2010) Diffusion-weighted magnetic resonance without bowel preparation for detecting colonic inflammation in inflammatory bowel disease. *Gut* 59:1056–1065
- Gahr N, Darge K, Hahn G et al (2011) Diffusion-weighted MRI for differentiation of neuroblastoma and ganglioneuroblastoma/ganglioneuroma. *Eur J Radiol* 79:443–446
- Low RN, Francis IR (1997) MR imaging of the gastrointestinal tract with i.v., gadolinium and diluted barium oral contrast media compared with unenhanced MR imaging and CT. *AJR* 169:1051–1059
- Del Vescovo R, Sansoni I, Caviglia R et al (2008) Dynamic contrast enhanced magnetic resonance imaging of the terminal ileum: differentiation of activity of Crohn's disease. *Abdom Imaging* 33:417–424
- Florie J, Wasser MN, Arts-Cieslik K et al (2006) Dynamic contrast-enhanced MRI of the bowel wall for assessment of disease activity in Crohn's disease. *AJR* 186:1384–1392
- Pauls S, Kratzer W, Rieber A et al (2003) [Quantifying the inflammatory activity in Crohn's disease using CE dynamic MRI] (in German). *Rofo* 175:1093–1099
- Umschaden HW, Szolar D, Gasser J et al (2000) Small-bowel disease: comparison of MR enteroclysis images with conventional enteroclysis and surgical findings. *Radiology* 215:717–725
- Martinez MJ, Ripolles T, Paredes JM et al (2009) Assessment of the extension and the inflammatory activity in Crohn's disease: comparison of ultrasound and MRI. *Abdom Imaging* 34:141–148
- Dillman JR, Ladino-Torres MF, Adler J et al (2011) Comparison of MR enterography and histopathology in the evaluation of pediatric Crohn disease. *Pediatr Radiol* 41:1552–1558
- Bilgili MY (2012) Reproducibility of apparent diffusion coefficients measurements in diffusion-weighted MRI of the abdomen with different b values. *Eur J Radiol* 81:2066–2068